Controllable Raman soliton self-frequency shift in nonlinear metamaterials

Yuanjiang Xiang, Xiaoyu Dai, Shuangchun Wen, Jun Guo, and Dianyuan Fan

Phys. Rev. A **84**, 033815 — Published 12 September 2011

DOI: 10.1103/PhysRevA.84.033815

Controllable Raman soliton self-frequency shift in nonlinear metamaterial

Yuanjiang Xiang,[1,*] Xiaoyu Dai,[2] Shuangchun Wen,[1,†] Jun Guo,[1] and Dianyuan Fan[1]

[1]*Laboratory for Micro/Nano Optoelectronic Devices of Ministry of Education, School of Information Science and Engineering, Hunan University, Changsha 410082, China*

[2]*College of Electrical and Information Engineering, Hunan University, Changsha 410082, China*

(Dated: August 9, 2011)

Abstract

Controllable and dispersive magnetic permeability in the metamaterials (MMs) provide us more freedoms to harness the propagation of ultrashort electromagnetic pulses at will. Here we discuss the controllability of the Raman soliton self-frequency shift (SSFS) in the MMs with a nonlinear electric polarization. First, we derive a generalized nonlinear Schrödinger equation suitable for few-cycle pulse propagation in the MMs with delayed Raman response, and demonstrate the Raman, high-order Raman and high-order nonlinear dispersion terms occurring in this equation. Second, we present a theoretical investigation on the controllability of the Raman SSFS in the MMs. Particularly, we identify the combined effects of the anomalous self-steepening (SS), third-order dispersion (TOD) and Raman scattering on SSFS. It is shown that the positive SS effect suppresses SSFS, however the negative SS effect enhances SSFS, and the positive TOD leads to the deceleration of SSFS. Finally, the effects of SS and TOD on the SSFS of the second-order soliton are also discussed.

PACS numbers: 42.81.Dp, 41.20.Jb, 78.67.Pt, 78.20.Ci

*Electronic address: xiangyuanjiang@126.com

†Electronic address: scwen@vip.sina.com

I. INTRODUCTION

Metamaterials (MMs) are artificial structures that display properties beyond those available in naturally occurring materials [1, 2]. MMs host a number of unusual properties [3], and the controllable optical magnetic responses are essential for various applications such as perfect len [4], superlen [5, 6], subwavelength waveguides and antennas [7, 8], and electromagnetic cloaking devices [9, 10]. Recently, the realizability of the optical MMs [1, 11, 12] and achievable nonlinear MMs [13, 14] have stimulated many investigations on the nonlinear optical properties of the MMs. Especially, the rich and novel linear and nonlinear electromagnetic properties enable MMs to be new but potential candidate for stable soliton and other nonlinear phenomena. The electromagnetic (EM) pulse propagation equation in the nonlinear MMs has been proposed, including the nonlinear interaction of ultrashort pulse with MMs [15–19], modulation instability (MI) [20–22] and optical soliton [23, 24]. It is found that the linear and nonlinear coefficients of the propagation equations in the MMs can be tailored through tuning the linear properties of the MMs to attain any combination of signs unachievable in ordinary matter, and shown significant potential to realize a wide class of solitary waves and ultrashort pulse propagation [20–22]. It is also indicated that negative refraction not only brings some new features to MI, but also makes MI possible, which is otherwise impossible in ordinary material [20–22]. Furthermore, the dispersive magnetic permeability generates more new nonlinear effects, including the anomalous self-steepening (SS) effect, second-order nonlinear dispersion and other high-order nonlinear dispersion. Particularly, the anomalous SS effect and second-order nonlinear dispersion lead to the significant changes of the conditions for the MI and soliton, comparing with the case in an ordinary positive-index material. Hence, the controllable nonlinear MMs will provide us more freedoms to manipulate the ultrashort pulse and soliton.

In the present paper, we intend to give a systematic investigation of the Raman Soliton self-frequency shift (SSFS) phenomenon associated with the novel optical properties of the MMs. SSFS is a well known nonlinear phenomenon that the mean frequency of the short pulse undergoes a continual redshift, which is induced by the Stimulated Raman scattering (SRS) effect. Because of SRS effect, the energy of the short pulse is continuously transferred from higher to lower frequency components so that the whole spectrum moves toward the longer wavelength region during the propagation in the nonlinear material. In 1986, Mitschke

et al. [25] firstly observed the SSFS in the optical fiber , then the theoretic analysis was given by Gordon [26] in the same year. Since then SSFS has been investigated extensively in the various optical fibers [27], and many applications are demonstrated including supercontinuum generation [28], femtosecond pulse sources [29], analog-to-digital conversion [30] and signal processing [31]. Hence, it is very important to manipulate the SSFS in different conditions. For this purpose, various methods have been proposed to control SSFS, including suppressing the SSFS by bandwidth-limited amplification [32–34], cross-phase modulation [35], upshifted filtering [36], negative dispersion slope [37] and self-steepening (SS) [38] or enhancing the SSFS by reducing the initial pulse width [39], optimizing the photonic crystal fibers [40, 41]. However, the ability to manipulate SSFS by using conventional nonlinear materials is limited. Unique EM properties of the MMs will provide an opportunity for harnessing SSFS, including both enhancing or suppressing SSFS.

Our focus is on the investigation of the controllability of Raman SSFS in nonlinear MMs. But, so far, the propagation characteristics of ultrashort EM pulse propagation in nonlinear MMs with delayed Raman response are not clearly revealed. Only the competition between Raman term and SS effect is investigated [24]. To unfold the role of the dispersion magnetic permeability on Raman scattering term and demonstrate the controllability of Raman SSFS in nonlinear MMs, in Sec. II, we give a simple derivation for the generalized nonlinear Schrödinger equation (NLSE) suitable for few-cycle pulse propagation in the MMs. Then, the linear and nonlinear characterization parameters described by Drude model are discussed in Sec. III.A. In Sec. III. B, by utilizing the standard split-step Fourier method, the physical mechanism of the controllable SSFS in the nonlinear MMs is investigated. Finally, the results achieved are summarized in Sec. IV.

II. THEORETICAL MODEL FOR EM PULSE PROPAGATION IN NONLINEAR MMS WITH DELAYED RAMAN RESPONSE

Two major theoretical models have been considered so far to describe the physics of the EM pulse propagation in the nonlinear MMs. The first model is the envelope equation of the nonlinear Schrödinger type, which reduces the second-order wave equation for the EM field to a simple first-order NLSE for the envelope. In the framework of the slowing varying envelope approximation (SVEA), generalized NLSEs for EM pulse propagation in the MMs

with both nonlinear electric polarization and nonlinear magnetization are presented [17–19]. However, the NLSE in the framework of SVEA can be applied only to the EM pulse whose temporal envelope changes slowly as compared with an optical cycle, and it will be broke down even for initial pulses that are many optical cycles long [42]. Going beyond the usual SVEA, Scalora et al. [15] investigated the propagation of EM pulses at least a few tens of optical cycles in MMs. After that, Wen et al. [20, 21] obtained a more general NLSE suitable for few-cycle pulse propagation in MMs.

The second model is the unidirectional optical pulse propagation equation (UPPE) for EM field [43, 44]. Abandoning the envelope concept and operating directly with pulse field, Kinsler has derived the UPPE for the materials with both electric and magnetic dispersion and nonlinearity based on the directional field approach [44]. This requires only a single, well-defined approximation to reduce a one-dimensional bidirectional forward-backward coupled model down to a unidirectional first-order wave equation. The importation approximation is that the pulse evolves only slowly on the scale of a wavelength, which is remarkably robust for all physically realistic parameter values [45]. UPPE is proposed firstly by Kolesik et al. to provide a seamless transition form Maxwell's equation to the various envelope-based models [46, 47]. This approach has no intrinsic bandwidth restrictions, makes no demands on the pulse profile, allows for an arbitrary dispersion, and does not require a co-moving frame. And that the NLSE previously published can be derived from the UPPE so long as we select appropriate additional approximations in the UPPE [43, 44, 48].

In order to obtain the propagation equation in the nonlinear MMs with the delayed Raman response, we generalize the derivation of the NLSE based on our works previously [20–22]. We assume that the pulse is propagating in uniform, bulk material, in which there are no free charges and no free currents flow, and under the condition of a nonlinear polarization [13]. To describe electromagnetic fields propagating in dispersive MMs, we start with Maxwell equations, $\nabla \times \mathbf{E} = -\partial_t \mathbf{B}$, $\nabla \times \mathbf{H} = \partial_t \mathbf{D_L} + \partial_t \mathbf{P_{NL}}$, $\nabla \cdot \mathbf{D} = 0$ and $\nabla \cdot \mathbf{B} = 0$, where $\mathbf{E}$ and $\mathbf{H}$ are electric and magnetic fields, respectively, and $\mathbf{D}$ and $\mathbf{B}$ are electric and magnetic flux densities. $\mathbf{D} = \mathbf{D_L} + \mathbf{P_{NL}}$, $\mathbf{D_L} = \varepsilon \mathbf{E}$, $\mathbf{B} = \mu \mathbf{H}$, with ε and μ being the medium permeability and permeability respectively, $\mathbf{P}_{NL}$ is the nonlinear polarization which is assumed to be related to the electric field by the relation

$$\mathbf{P}_{NL}(\mathbf{r}, t) = \varepsilon_0 \chi^{(3)} \mathbf{E}(\mathbf{r}, t) \int_{-\infty}^{t} R(t - t_1) |\mathbf{E}(\mathbf{r}, t_1)|^2 dt_1, \tag{1}$$

where it is assumed that the electric and the induced polarization vectors point along the same direction. $\chi^{(3)}$ is the third-order susceptibility, $R(t)$ is the Raman response function [49]. In the present paper, we focus on the influence of the linear and nonlinear EM properties on the SSFS, hence we assume that the Raman response function in the MMs has the similar form as that in the optical fiber.

It is convenient to work in the frequency domain to deal with the problem of pulse propagation in the dispersive medium. From the Maxwell equations we can obtain the following wave equation in frequency domain,

$$\frac{\partial^2 \tilde{E}\left(z,\omega\right)}{\partial z^2} = \omega^2 \mu \varepsilon \tilde{E}\left(z,\omega\right) + \omega^2 \mu \tilde{P}_{NL}. \tag{2}$$

For simplicity, we consider one longitudinal spatial coordinate and time. And we assume that the electric field $\mathbf{E}$ propagates along the z directional, and both $\mathbf{E}$ and nonlinear polarization $\mathbf{P_{NL}}$ are polarized parallel to the x axis. In addition, we assume the transverse inhomogeneities of the medium polarization to be small. The tilde variables stand for the Fourier transform of the corresponding untilde variables.

The purpose to transform Maxwell's equations in temporal domain into frequency space is that in frequency space we can expand $\epsilon(\omega)$ and $\mu(\omega)$ in powers of ω, thus enabling us to treat the material parameters as a power series which we can truncate to an appropriate order. However for simplicity it is better to expand $\omega\epsilon(\omega)$ and $\omega\mu(\omega)$ about a suitable ω_0 instead,

$$\omega\varepsilon(\omega) = \sum_{m=0}^{\infty}\left[\frac{F_m}{m!}(\omega-\omega_0)^m\right], \tag{3}$$

$$\omega\mu(\omega) = \sum_{m=0}^{\infty}\left[\frac{G_m}{m!}(\omega-\omega_0)^m\right], \tag{4}$$

where $F_m = \partial^m\left[\omega\varepsilon(\omega)\right]/\partial\omega^m|_{\omega=\omega_0}$, $G_m = \partial^m\left[\omega\mu(\omega)\right]/\partial\omega^m|_{\omega=\omega_0}$. Substituting Eqs. (3) and (4) into Eq. (2), we have

$$\frac{\partial^2\tilde{E}}{\partial z^2} = -\sum_{m=0}^{\infty} d_m(\omega-\omega_0)^m\tilde{E} - \omega\sum_{m=0}^{\infty}\frac{G_m}{m!}(\omega-\omega_0)^m\tilde{P}_{_{NL}}, \tag{5}$$

where $d_m = \sum_{l=0}^{m} F_l G_{m-l}/\left[l!\left(m-l\right)!\right]$.

We introduce an envelope and carrier form for the field in the usual way, $E(z,t) = (1/2)A(z,t)\exp\left(ik_0z - i\omega_0t\right) + c.c$, where k_0 is the wave number and ω_0 is the carrier frequency. With this envelope-carrier substitution and taking the inverse Fourier transform of

Eq. (5), the propagation equation in the moving reference frame $T = t - z/v_g$, $Z = z$, is

$$\frac{\partial A}{\partial Z} = -\frac{i\beta_2}{2}\frac{\partial^2 A}{\partial T^2} + \sum_{m=3}^{\infty}\frac{i^{m+1}\delta_m}{m!}\frac{\partial^m A}{\partial T^m} + \frac{i}{2k_0}\left(\frac{\partial^2 A}{\partial Z^2} - \frac{2}{v_g}\frac{\partial^2 A}{\partial T \partial z}\right) + \sum_{m=0}^{\infty}\frac{i^{m+1}\gamma_m}{m!}\frac{\partial^m}{\partial T^m}\left(1 + \frac{i}{\omega_0}\frac{\partial}{\partial T}\right)\left[A(Z,T)\int_{-\infty}^{\infty} R(T')\left|A(Z,T-T')\right|^2 dT'\right]. \quad (6)$$

where $v_g = 2k_0/(F_0G_1 + F_1G_0)$ is the group velocity, $\beta_2 = \delta_2 - \left(k_0 v_g^2\right)^{-1}$ is group velocity dispersion (GVD), $\delta_m = m!d_m/(2k_0)$ and $\gamma_m = \omega_0\chi G_m/(2k_0)$ characterize the dispersive and nonlinear properties of the material, respectively. We have not made any further approximations in the derivation of Eq. (6), hence it is suitable for few-cycle pulses propagating in the MMs.

For pulses wide enough to contain many optical cycles, the convolution integral in Eq.(6) can be approximated by $|A|^2 - T_R\partial|A|^2/\partial T$, where T_R is the first moment of the Raman response function. We thus can simplify Eq. (6) to the following form

$$\frac{\partial A}{\partial Z} = -\frac{i\beta_2}{2}\frac{\partial^2 A}{\partial T^2} + \sum_{m=3}^{\infty}\frac{i^{m+1}\delta_m}{m!}\frac{\partial^m A}{\partial T^m} + \frac{i}{2k_0}\left(\frac{\partial^2 A}{\partial Z^2} - \frac{2}{v_g}\frac{\partial^2 A}{\partial T \partial Z}\right) + \sum_{m=0}^{\infty}\frac{i^{m+1}\gamma_m}{m!}\frac{\partial^m}{\partial T^m}\left(1 + \frac{i}{\omega_0}\frac{\partial}{\partial T}\right)\left(|A(Z,T)|^2 A - T_R A\frac{\partial|A|^2}{\partial T}\right), \quad (7)$$

We now calculate the first order non-SVEA correction terms by using Eq. (7) to evaluate $\partial^2 A/\partial Z^2$ and $\partial^2 A/\partial T\partial Z$ [15]. Neglecting the dispersion terms higher than second-order and higher order nonlinear terms,

$$\frac{\partial^2 A}{\partial Z^2} \approx -\frac{\beta_2^2}{4}\frac{\partial^4 A}{\partial T^4} - \gamma_0^2|A|^4 A + \frac{\gamma_0\beta_2}{2}\frac{\partial^2}{\partial T^2}\left(|A|^2 A\right) - \frac{\gamma_0\beta_2}{2}A^2\frac{\partial^2 A^*}{\partial T^2} + \gamma_0\beta_2|A|^2\frac{\partial^2 A}{\partial T^2}, \quad (8)$$

$$\frac{\partial^2 A}{\partial T\partial Z} \approx -\frac{i\beta_2}{2}\frac{\partial^3 A}{\partial T^3} + i\gamma_0\frac{\partial}{\partial T}\left(|A|^2 A\right). \quad (9)$$

Inserting Eqs. (8) and (9) in Eq. (7), keeping the dispersion terms to third order and the nonlinear terms to second order derivatives of time, we finally obtain the propagation equation first order in the propagation distance

$$\frac{\partial A}{\partial Z} = -\frac{i\beta_2}{2}\frac{\partial^2 A}{\partial T^2} + \frac{\beta_3}{6}\frac{\partial^3 A}{\partial T^3} + i\gamma_0|A|^2 A - i\gamma_0\sigma|A|^4 A - \gamma_0 S_1\frac{\partial}{\partial T}\left(|A|^2 A\right) - i\gamma_0 S_2\frac{\partial^2}{\partial T^2}\left(|A|^2 A\right) - i\gamma_0 T_R A\frac{\partial|A|^2}{\partial T} - \gamma_0 T_R'\frac{\partial}{\partial T}\left(A\frac{\partial|A|^2}{\partial T}\right) + i\gamma_0\eta\left(2|A|^2\frac{\partial^2 A}{\partial T^2} - A^2\frac{\partial^2 A^*}{\partial T^2}\right), \quad (10)$$

where $\beta_3 = \delta_3 - 3\beta_2/(k_0 v_g)$ is the third-order dispersion (TOD), $\sigma = \gamma_0/(2k_0)$ is saturation nonlinearity, $S_1 = 1/\omega_0 + \gamma_1/\gamma_0 - (k_0 v_g)^{-1}$ and $S_2 = \gamma_1/(\omega_0\gamma_0) - \beta_2/(4k_0) + \gamma_2/(2\gamma_0)$ are SS and second order nonlinear dispersive coefficients, respectively, $T_R' = -(1/\omega_0 + \gamma_1/\gamma_0)\, T_R$ is second order Raman effect coefficient, and $\eta = \beta_2/(4k_0)$ is the complex higher order nonlinear coefficient. It can be found that the Raman scattering term is not influenced by the properties of the MMs, however the high-order Raman effect coefficients will be influenced by the dispersive magnetic permeability of the MM. These properties will provide us more methods to control the propagation of the soliton and ultrashort pulse.

III. THE CONTROLLABLE RAMAN SOLITON SELF-FREQUENCY SHIFT IN METAMATERIALS

To specially elucidate the Raman SSFS in MMs, we keep the linear dispersion terms to the third order, only keep the first order time derivative of nonlinearity terms and neglect the fifth-order nonlinearity. Thus Eq. (10) becomes

$$\frac{\partial A}{\partial z} = -\frac{i\beta_2}{2}\frac{\partial^2 A}{\partial T^2} + \frac{\beta_3}{6}\frac{\partial^3 A}{\partial T^3} + i\gamma_0[|A|^2 A + iS_1\frac{\partial}{\partial T}\left(|A|^2 A\right) - T_R A\frac{\partial |A|^2}{\partial T}], \tag{11}$$

This simplified equation has the same form as that in Ref. [24]. It can also be derived from the UPPE [44] so long as we make appropriate additional approximations. For the purposes of computations, it is convenient to rewrite Eq. (11) in normalized units. Introducing the normalized variables $\tau = T/T_p, \xi = Z/|l_{d2}|$, and $U = A/A_0$, where T_p is the duration of the input pulse, A_0 is the amplitude of the input field, and defining the mth-order dispersion length, $L_{dm} = T_p^m/\beta_m$, the nonlinear length, $L_{nl} = (\gamma_0 A_0^2)^{-1}$, we can transform Eq. (11) into the normalized form

$$\partial_\xi U = -\frac{isgn(\beta_2)}{2}\partial_\tau^2 U + \frac{b_3}{6}\partial_\tau^3 U + i\vartheta N^2\left[|U|^2 U + is_1\partial_\tau\left(|U|^2 U\right) - \tau_R U\partial_\tau |U|^2\right]. \tag{12}$$

where $\vartheta = \pm 1$ for focusing and defocusing nonlinearity respectively; $N^2 = |L_{d2}|/|L_{nl}|$, N is the soliton-order; $b_3 = |L_{d2}|/L_{d3}$, $s_1 = S_1/T_p$, $\tau_R = T_R/T_p$. Clearly, as the pulse duration T_p decreases, s_1 and τ_R increase, meaning that the SS and Raman effects become more important, like the linear dispersion.

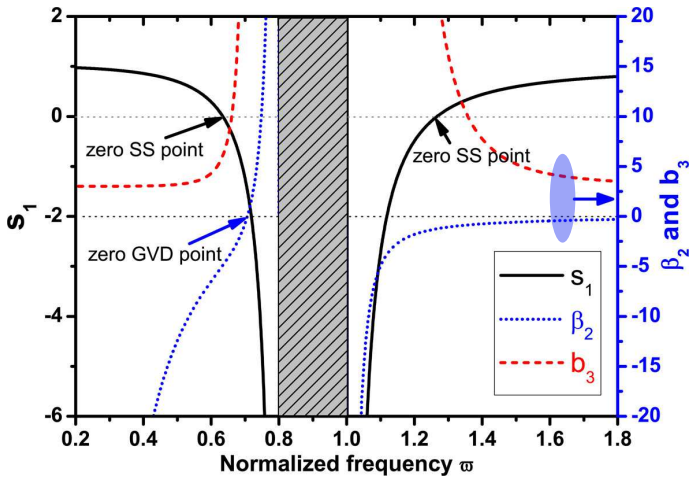

FIG. 1: (Color Online) SS coefficient s_1, GVD parameter β_2, normalized TOD parameter b_3 versus $\tilde{\omega}$ for $\omega_{pm}/\omega_{pe} = 0.8$. β_2 is calculated in units of $1/(c\omega_{pe})$, s_1 and b_3 in units of s.

A. The properties of metamaterial described by Drude model

For an ideal lossless MMs, the frequency dispersion $\varepsilon_r(\omega)$ and $\mu_r(\omega)$ can be described by the Drude model [4], $\varepsilon_r = 1-\omega_{pe}^2/\omega^2, \mu_r = 1-\omega_{pm}^2/\omega^2$, where ω_{pe} and ω_{pm} are the respective electric and magnetic plasma frequencies. For simplicity, we introduce scaled frequencies, $\tilde{\omega} = \omega/\omega_{pe}, \tilde{\omega}_p = \omega_{pm}/\omega_{pe}$. Thus the refractive index is $n = \sqrt{1-1/\tilde{\omega}^2}\sqrt{1-\tilde{\omega}_p^2/\tilde{\omega}^2}$, the group velocity is $v_g = nc/(1-\tilde{\omega}_p^2/\tilde{\omega}^4)$, and the GVD and TOD are

$$\beta_2 = \frac{1}{\omega_{pe}cn\tilde{\omega}}\left\{\left(1+3\tilde{\omega}_p^2\tilde{\omega}^{-4}\right) - \frac{1}{n^2}\left(1-\tilde{\omega}_p^2\tilde{\omega}^{-4}\right)^2\right\}, \tag{13}$$

$$\beta_3 = -\frac{12\tilde{\omega}_p^2}{nc\omega_{pe}^2\tilde{\omega}^6} - \frac{3\beta_2\left(\tilde{\omega}^4-\tilde{\omega}_p^2\right)}{\omega_{pe}n^2\tilde{\omega}^5}. \tag{14}$$

Then the normalized TOD coefficient and SS coefficient are

$$b_3 = \mathrm{sgn}\left(\beta_3\right) s\left|\frac{12\tilde{\omega}_p^2\tilde{\omega}^{-4}}{\left(1+3\tilde{\omega}_p^2\tilde{\omega}^{-4}\right) - n^{-2}\left(1-\tilde{\omega}_p^2\tilde{\omega}^{-4}\right)^2} + \frac{3\left(\tilde{\omega}^4-\tilde{\omega}_p^2\right)}{n^2\tilde{\omega}^4}\right|, \tag{15}$$

$$s_1 = s\left(1+\frac{\tilde{\omega}_p^2-\tilde{\omega}^4}{n^2\tilde{\omega}^4} + \frac{\tilde{\omega}^2+\tilde{\omega}_p^2}{\tilde{\omega}^2-\tilde{\omega}_p^2}\right), \tag{16}$$

where $s = 1/(\omega_0 T_p)$. If we assume that $\omega_{pe} > \omega_{pm}$, we know that in Drude model, MMs can be divided into three regions: (1) in the spectral interval $\omega_{pm} < \omega < \omega_{pe}$, the linear electromagnetic waves are evanescent ($k^2(\omega) < 0$). This is a band gap, where $\mu_r(\omega) > 0$ but $\varepsilon_r(\omega) < 0$. (2) negative-index region with $\omega < \omega_{pm}$, and (3) positive-index region with

$\omega > \omega_{pe}$. Moreover, to disclose the parameters characteristics in Eq. (12), we have plotted the variation of β_2, b_3 and s_1 in Fig. 1 for $\tilde{\omega}_p = 0.8$. β_2 is calculated in units of $1/(c\omega_{pe})$, and b_3 and s_1 in units of s. Obviously, in the negative-index region, β_2 and s_1 can be either positive or negative, the zero GVD point and zero SS point are located at $\tilde{\omega} \approx 0.709$ and 0.634 respectively. While in the positive-index region, β_2 is always positive, but s_1 can be either positive or negative with the second zero SS point occurring. In both regions, b_3 is always positive. Furthermore, by controlling the structure parameters of MMs, the zero GVD point can be shifted back and forth, and the SS and TOD can also be engineered.

B. Raman soliton self-frequency shift in the nonlinear MMs

Now, we discuss the Raman SSFS in the MMs. To disclose the roles of SS and TOD in the SSFS, we numerically solve Eq. (12) using the standard split-step Fourier method for $\tilde{\omega}_p = 0.8$ in the case of self-focusing nonlinearity. In our early article [20], we have found that the negative SS moves the center of soliton toward the leading side, opposite to the case of positive SS. Recently, Boardman et al. [23, 24] show that the negative SS can be used to combat Raman scattering, however the influences of anomalous SS on the Raman SSFS are still unfolded. We will particularly concern about the Raman SSFS in the negative-index region due to the novel properties of the electromagnetic pulse propagating in this region, and the results in the positive-index region can be disposed similarly. In the negative-index region, SS coefficient can be positive, negative or zero, we choose three typical values $s_1 = 0, 0.2$ and -0.2 in the simulation. Moreover, the typical Raman coefficient $\tau_R = 0.1$ is assumed. An ideal optical soliton,

$$A(T, z = 0) = \mathrm{A_0 Sech}(T/T_p), \tag{17}$$

is defined as the input pulse, where A_0 is the soliton amplitude and T_p is the pulse width. In the simulations, we adopt the normalized amplitude and width, assume that the input pulse is $U(\tau, \xi = 0) = \mathrm{Sech}(\tau)$. First, we focus on the effects of the anomalous SS on the SSFS, and neglect the effect of TOD. To disclose the interplay between SS and Raman scattering, we show the time evolution of the fundamental soliton (N=1) in different SS coefficients for $\tau_R = 0.1$ in the Fig. 2. The output pulse at $\xi = 30$, is shown in Fig. 2(a), it seems to indicate that the negative SS effect accelerates the movement toward the back of the pulse,

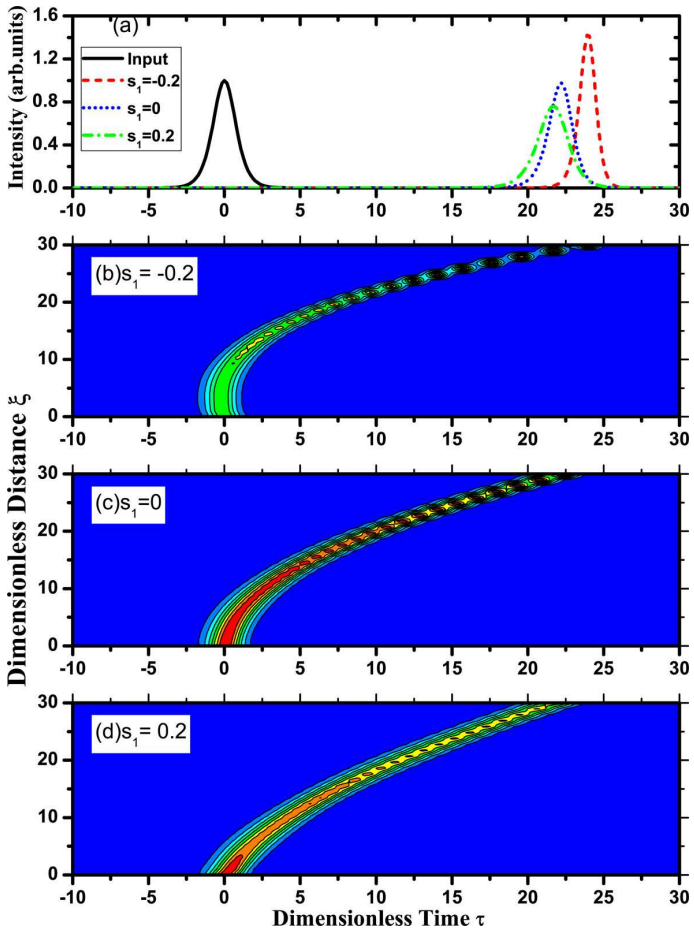

FIG. 2: (Color Online) Time evolution of the fundamental soliton in different SS coefficients in the anomalous GVD.(a)The output pulse intensity at the normalized distance $\xi = 30$, the input pulse is also indicated in solid line; (b), (c) and (d) are the contour maps of the pulse evolution for $s_1 = -0.2, 0$ and 0.2, respectively. Here, $\tau_R = 0.1$

and positive SS coefficient decelerates the movement. To disclose the interplay for the MMs between SS effect and Raman scattering, in Fig. 2(b)-(d), we have plotted the contour maps of the pulse evolution for $s_1 = -0.2, 0$ and 0.2, respectively. If we neglect the SS effect and only consider the Raman Scattering, as shown in Fig. 2(c), it is found that Raman scattering moves the soliton toward the back of the pulse. However, in our early work [20], we have shown that the negative SS effect moves the pulse to the leading sides, opposite to the case of positive SS. Obviously, here is a process of competition between the negative SS effect and Raman scattering effect. The SS effect prevails within a short distance, leading to the movement toward the front of the pulse, as the propagation distance is increasing ,

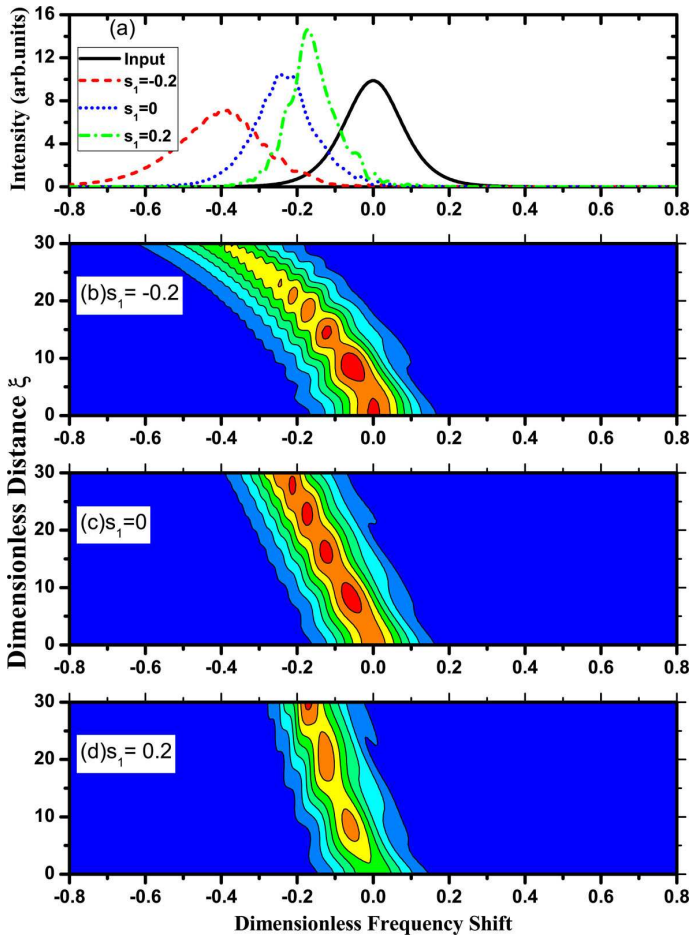

FIG. 3: (Color Online) Spectra evolution of the fundamental soliton in different SS coefficients in the anomalous GVD.(a)The output pulse spectra at the normalized distance $\xi = 30$; (b), (c) and (d) are the contour maps of the spectra evolution for $s_1 = -0.2, 0$ and 0.2, respectively. Here, $\tau_R = 0.1$

Raman scattering is gradually beginning to occupy the dominant role and shift the soliton to trailing sides, as shown in Fig. 2(b). Moreover, the positive SS effect and Raman scattering both act to accelerate the movement toward the trailing sides, as shown in Fig. 2(d). At the longer distances, the behaviors of the soliton evolution become very complex due to the interplay of the SS effect and Raman scattering term, but we find that negative SS effect actually accelerates the movement toward the trailing edges, opposite to the case of the positive SS effect.

Now, let's check the influences of the SS effect on the SSFS. Fig. 3 shows the soliton evolution spectrum of the fundamental soliton for different SS coefficients. It is clear that

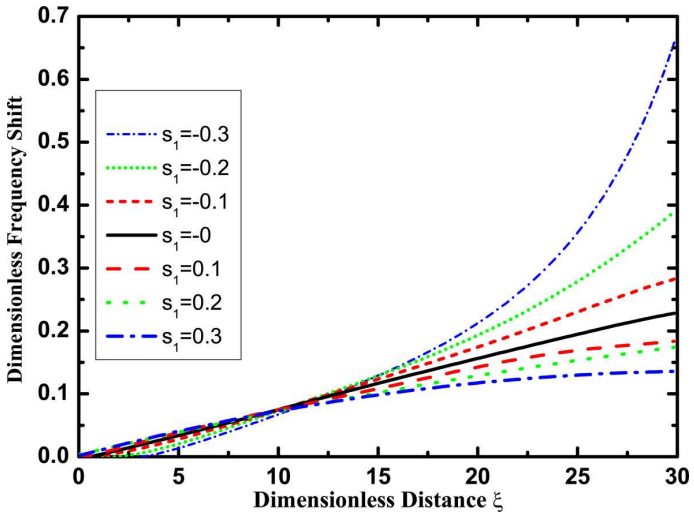

FIG. 4: (Color Online) SSFS fitted as a function of the propagation distance for different SS coefficients, $\tau_R = 0.1$.

the positive SS decelerates SSFS, as shown in Fig. 3(d), this result is very close agree with the prediction by Voronin et al [38] in the conventional optical fiber. But there is still no correlative work for the role of the negative SS effect in the SSFS. As seen from Fig. 3(b), we find that the frequency shift is enhanced markedly by the negative SS effect, meanwhile the spectra are widened as shown in Fig. 3(a). These results show that the negative SS effect has a valuable potential for supercontinuum generation and broadband source. Moreover, the engineerable linear and nonlinear electromagnetic properties of MMs allow us to manipulate the SS coefficient elaborately, and this controllable SS effect causes the engineerable Raman SSFS. To demonstrate this, in Fig. (4) we compare the SSFS fitted as the propagation distance for different SS coefficients from positive to negative values. Within the long propagation distance, it is straightforward to see that the positive SS effect suppresses the SSFS, and the frequency movements display a dramatic deceleration and become saturated gradually as the propagation distance increased. The larger the positive SS coefficient is, the less the frequency shifts when $\xi > 15$. However, the negative SS effect shifts the soliton spectra toward the lower frequency constantly with the increasing propagation distance, and the larger the absolute values of the negative SS coefficient is, the greater the frequency shifts when $\xi > 15$. The frequency shifts for $s_1 = -0.3$ are almost three times as the frequency shifts without considering the SS effect at $\xi = 30$. Therefore, we can obtain arbitrary SSFS as we expected by manipulating the SS effect in MMs.

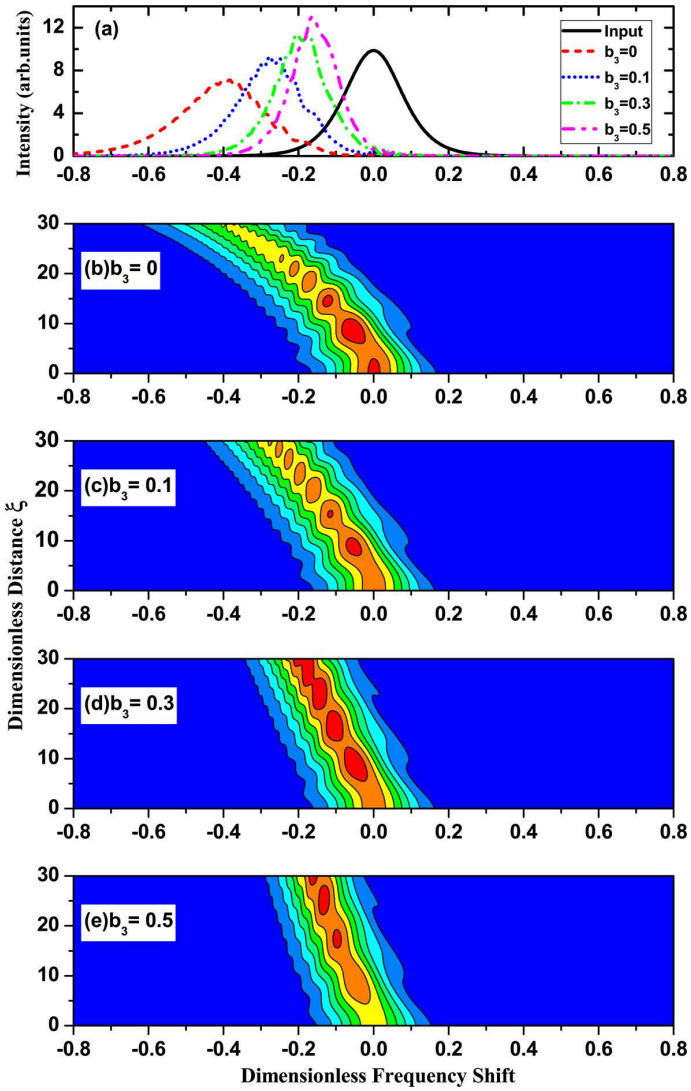

FIG. 5: (Color Online) Spectra evolution of the fundamental soliton in different TOD in the anomalous GVD. (a)The output pulse spectra at the normalized distance $\xi = 30$; (b), (c), (d) and (e) are the contour maps of the spectra evolution for $b_3 = 0, 0.1, 0.3$ and 0.5, respectively. Here, $\tau_R = 0.1$, $s_1 = -0.2$.

In the above discussions, TOD has been neglected. However, normalized TOD coefficient β_3 is inversely proportional to the pulse width T_p, hence TOD becomes necessary for few-cycle pulses. Fig. 5 shows the spectra evolution of the fundamental soliton in different TOD in the anomalous GVD, here we assume that $\tau_R = 0.1$,$s_1 = -0.2$. For the sake of contrast, we have chosen four TOD coefficients, $b_3 = 0, 0.1, 0.3$ and 0.5. TOD coefficient is always positive in the MMs described by the Drude model, which can be seen from Fig. 1. If $b_3 = 0$, the main peak shifts toward the leading side at a rapid rate with the increasing distance

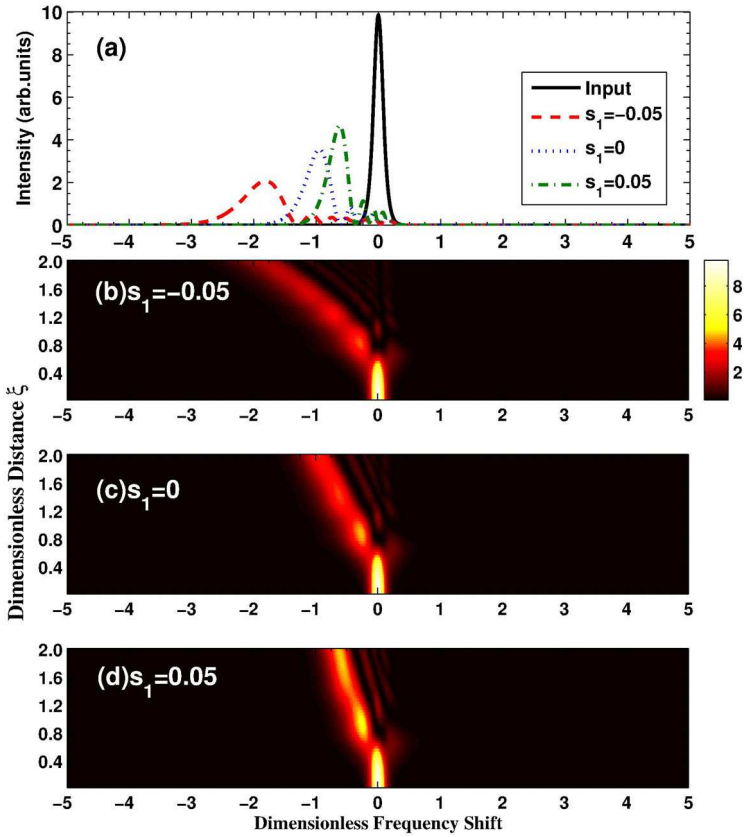

FIG. 6: (Color Online) Spectra evolution of the second-order soliton in different SS coefficient in the anomalous GVD. (a)The output pulse spectra at the normalized distance $\xi = 2$; (b), (c), and (d) are the contour maps of the spectra evolution for $s_1 = -0.05, 0$ and 0.05, respectively. Here, $\tau_R = 0.1$, $b_3 = 0$.

due to the interplay of the SS effect and Raman scattering, as shown in Fig. 5(a). However, when TOD is taken into consideration the main peak shift of the pulse is suppressed, as shown in Fig. 5 (b)-(e). Moreover, the frequency shift is decelerated with the increasing TOD coefficients. The frequency shift of the main peak at $b_3 = 0.5$ has been suppressed to the half of the frequency shift comparing with the case of neglecting the TOD coefficient.

Finally, we give a simple discussion about the interplay between the SS effect and Raman scattering on the higher-order solitons. Here, Fig. 6 shows such an example for a second-order soliton (N=2) by solving Eq. (12) numerically with $\tau_R = 0.1$ and three different SS coefficients $s_1 = -0.05, 0$ and 0.05. For high-order soliton, even relative small values of τ_R and s_1 will lead to the decay of higher-order soliton into its constituents at a very short

distance. For the spectra evolution of the second-order soliton, the comparison of Fig. 3 and Fig. 6 shows that even a small negative SS coefficient ($s_1 = -0.05$) has achieved relatively large frequency shift of the main peak. This shift is far greater than the frequency shift of the fundamental soliton at a larger negative SS coefficient ($s_1 = -0.2$). Like the frequency shift for the fundamental soliton, the negative SS coefficient enhances the SSFS and positive SS suppresses the SSFS. Another important difference seen between Fig. 3 and Fig. 6 is that the pulse spectrum of the second-order soliton evolves into several bands, and these trailing frequency bands also shift to lower frequency with the increasing propagation distance. Obviously, the negative SS coefficient leads to wider spectrum width, which suggests that the nonlinear MMs have valuable potentials for supercontinuum generation and broadband source.

IV. CONCLUSION

We have presented a theory to investigate the Raman SSFS in the nonlinear MMs. We derive a generalized NLSE suitable for few-cycle pulse propagation in the MMs with delayed Raman response, which is formally similar to the case of ordinary positive-index materials, but has an anomalous SS parameter, high-order Raman terms and high-order nonlinear dispersion. Then we show that the SSFS in nonlinear MMs with the controlled linear and nonlinear electromagnetic properties can be tailored. In particular, it is found that the negative SS term can enhance SSFS and the positive SS term will suppress SSFS within the long propagation distance. Moreover, we discuss the influence of TOD on SSFS, and show that TOD will decelerate the SSFS. Finally, the interplay between the anomalous SS effect and Raman scattering on the second-order soliton is discussed. For high-order soliton, we show that even relative small values of negative SS parameter can achieve relative large frequency shifts. Numerical calculations indicate that the negative SS coefficient leads to wider spectrum width, means that the nonlinear MMs are the valuable candidates for supercontinuum generation and broadband source.

ACKNOWLEGMENTS

This work was supported by projects of the National Natural Science Foundation of China (Grants Nos. 11004053, 10974049 and 61025024) and the Hunan Provincial Natural Science Foundation of China (Grant. 11JJB001).

---

[1] V. M. Shalaev,"Optical negative-index metamaterials," Nature Photonic, **1**, 41-48 (2007).

[2] D. R. Smith, W. J. Padilla, D. C. Vier, S. C. Nemat-Nasser, and S.Schultz, "Composite Medium with zimultaneously negative permeability and permittivity," Phys. Rev. Lett. **84**, 4184 (2000).

[3] V. G. Veselago, "The electrodynamics of substances with simultaneously negative values of ε and μ," Sov. Phys. Usp. **10**, 509(1968).

[4] J. B. Pendry, "Negative Refraction Makes a Perfect Lens," Phys.Rev. Lett. **85**, 3966 (2000).

[5] N. Fang, H. Lee, C. Sun, and X. Zhang, "Sub-diffaction-limited optical imaging with a silver superlens," Science. **308**, 534(2005).

[6] W. S. Cai , D. A. Genov , V. M. Shalaev, "Superlens based on metal-dielectric composites," Phys. Rev. B. **72**, 193101(2005).

[7] P. A. Belov and C. R. Simovski, "Subwavelength metallic waveguides loaded by uniaxial resonant scatterers," Phys. Rev. E, **72**, 036618(2005).

[8] N. Engheta, "An Idea for Thin Subwavelength Cavity Resonators Using Metamaterials With Negative Permittivity and Permeability," IEEE Antennas Wireless Propagat. Lett., **1**, 10-13 (2002).

[9] D. Schurig, J. J. Mock, B. J. Justice, S. A. Cummer, J. B. Pendry, A. F. Starr, and D. R. Smith, "Metamaterial electromagnetic cloak at microwave frequencies," Science, **314**, 977 (2006).

[10] W. S. Cai, U. K. Chettiar, A. V. Kildishev, V. M. Shalaev, "Optical cloaking with metamaterials," Nat. Photonics, **1**, 224-227 (2007).

[11] V. M. Shalaev, W. Cai, U. K. Chettiar, H. Yuan, A. K. Sarychev, V. P. Drachev, A. V. Kildishev, "Negative index of refraction in optical metamaterials." Opt. Lett., **30**, 3356 (2005).

[12] N. M. Litchinitser,and V.M. Shalaev, "Photonic metamaterials," Laser Phys. Lett., **5**, 411-420

(2008).

[13] A. A. Zharov, I. V. Shadrivov, and Y. S. Kivshar, "Nonlinear Properties of Left-Handed Metamaterials," Phys. Rev. Lett., **91**, 037401 (2003).

[14] M. Lapine, M. Gorkunov, and K. H. Ringhofer, "Nonlinearity of a metamaterial arising from diode insertions into resonant conductive elements," Phys. Rev. E, **67**, 065601 (2003).

[15] M. Scalora, M. S. Syrchin, N. Akozbek, E. Y. Poliakov, G. D'Aguanno, N. Mattiucci, M. J. Bloemer and A. M. Zheltikov, "Generalized nonlinear Schrödinger equation for dispersive susceptibility and permeability: application to negative index materials," Phys. Rev. Lett., **95**, 013902(2005).

[16] V. M. Agranovich, Y. R. Shen, R. H. Baughman and A. A. Zakhidov, "Linear and nonlinear wave propagation in negative refraction metamaterials," Phys. Rev. B, **69**, 165112 (2004).

[17] N. Lazarides and G. P. Tsironis, "Coupled nonlinear Schrödinger field equations for electromagnetic wave propagation in nonlinear left-handed materials," Phys. Rev. E, **71**, 036614 (2005).

[18] I. Kourakis and P. K. Shukla, "Nonlinear propagation of electromagnetic waves in negative-refraction-index composite materials," Phys. Rev. E, **72**, 016626 (2005).

[19] S. Wen, Y. Xiang, X. Dai, Z. Tang, W. Su, and D. Fan, "Theoretical models for ultrashort electromagnetic pulse propagation in nonlinear metamaterials," Phys. Rev. A, **75**, 033815 (2007).

[20] S. Wen, Y. Xiang, W. Su, Y. Hu, X. Fu, and D. Fan, "Role of the anomalous self-steepening effect in modulation instability in negative-index material," Opt. Express, **14**, 1568(2006).

[21] S. Wen, Y. Wang, W. Su, Y. Xiang, X. Fu, and D. Fan, "Modulation Instability in Nonlinear Negative-Index Material," Phys. Rev. E, **73**, 036617(2006).

[22] Y. Xiang, S. Wen, X. Dai, Z. Tang, W. Su, and D. Fan, "Modulation instability induced by nonlinear dispersion in nonlinear metamaterials," J. Opt. Soc. Am.B, **24**, 3058-3063 (2007).

[23] A. D. Boardman, N. King, R. C. Mitchell-thomas, V. Malnev, V. G. Rapoport, "Gain control and diffraction-managed solitons in metamaterials," Metamaterials, **2**, 145-154 (2008).

[24] A. D. Boardman, O. hess, R. C. Mitchell-thomas, Y. G. Rapoport, and L. Velasco, "Temporal solitons in magnetooptic and metamaterial waveguides," Photonics and Nanostructures, **8**, 228-243 (2010).

[25] F. M. Mitschke and L. F. Mollenauer, "Discovery of the soliton self-frequency shift," Opt.

Lett., **11**, 659 (1986).

[26] J. P. Gordon, "Theory of the soliton self-frequency shift," Opt. Lett., **11**, 662 (1986).

[27] J. H. Lee, J. V. Howe, C. Xu, and X. Liu, "Soliton Self-Frequency Shift: Experimental Demonstrations and Applications," IEEE J. Sel. Topics Quantum Electron, **14**, 713-723 (2008).

[28] J. M. Dudley, G. Genty, and S. Coen, "Supercontinuum generation in photonic crystal fiber," Rev. Mod. Phys, **78**, 1135 (2006).

[29] N. Nishizawa and T. Goto, "Compact system of wavelength-tunable femtosecond soliton pulse generation using optical fibers," IEEE Photon. Technol. Lett., **11**, 325-327 (1999).

[30] C. Xu and X. Liu, "Photonic analog-to-digital converter using soliton self-frequency shift and interleaving spectral filters," Opt. Lett., **28**, 986-988 (2003).

[31] M. Kato, K. Fujiura, and T. Kurihara, "Asynchronous all-optical bitby-bit self-signal recognition and demultiplexing from overlapped signals achieved by self-frequency shift of Raman soliton," Electron. Lett., **40**, 381-382 (2004).

[32] K. J. Blow, N. J. Doran, and David Wood, "Suppression of the soliton self-frequency shift by bandwidth-limited amplification," J. Opt. Soc. Am. B, **5**, 1301 (1988).

[33] A. S. Gouveia-Neto, A. S. L. Gomes, and J. R. Taylor, "Suppression and manipulation of the soliton self-frequency shift," Opt. Lett, **14**, 514 (1989).

[34] I. M. Uzunov, "Description of the suppression of the soliton self-frequency shift by bandwidth-limited amplification," Phy. Rev. E, **82**, 066603 (2010).

[35] D. Schadt and B. Jaskorzynska, "Suppression of the Raman self-frequency shift by cross-phase modulation," J. Opt. Soc. Am. B, **5**, 2374-2378 (1988).

[36] P. T. Dinda, K. Nakkeeran, and A. Labruy??re, "Suppression of soliton self-frequency shift by upshifted filtering," Opt. Lett., **27**, 382-384 (2002).

[37] D. V. Skryabin, F. Luan, J. C. Knight, P. St. J. Russell, "Soliton self-frequency shift cancellation in photonic crystal fibers," Science, **301**, 1705-1708 (2003).

[38] A. A. Voronin and A. M. Zheltikov, "Soliton self-frequency shift decelerated by self-steepening," Opt. Lett., **33**, 1723-1725 (2008).

[39] E. E. Serebryannikov, M. L. Hu, Y. F. Li, C. Y. Wang, Z. Wang, L. Chai, and A. M. Zheltikov, "Enhanced soliton self-frequency shift of ultrashort light pulses,"JETP Letters., **81**, 487-490(2005).

[40] R. Pant, A. C. Judge, E. C. Magi, B. T. Kuhlmey, M. de Sterke, and B. J. Eggleton, "Char-

acterization and optimization of photonic crystal fibers for enhanced soliton self-frequency shift,"J. Opt. Soc. Am. B, **27**, 1894-1901 (2010).

[41] A. C. Judge, O. Bang, B. J. Eggleton, B. T. Kuhlmey, E. C. Mägi, R. Pant, and C. M. de Sterke, "Optimization of the soliton self-frequency shift in a tapered photonic crystal fiber,"J. Opt. Soc. Am. B, **26**, 2064-2071 (2009).

[42] J. K. Ranka and A. Gaeta, "Breakdown of the slowly varying envelope approximation in the self-focusing of ultrashort pulses ," Opt. Lett., **23**, 534 (1998).

[43] P. Kinsler, "Optical pulse propagation with minimal approximations," Phys. Rev. A, **81**, 013819(2010).

[44] P. Kinsler, "A uni-directional optical pulse propagation equation for materials with both electric and magnetic responses," Phys. Rev. A, **81**, 023808(2010).

[45] P. Kinsler, "Limits of the uni-directional pulse propagation approximation," J. Opt. Soc. Am. B, **24**, 2363(2007).

[46] M. Kolesik, J. V. Moloney, and M. Mlejnek, "Unidirectional optical pulse propagation equation," Phys. Rev. Lett., **89**, 283902(2002).

[47] M. Kolesik and J. V. Moloney, "Nonlinear optical pulse propagation simulation: From Maxwell??s to unidirectional equations," Phys. Rev. E, **70**, 036604(2004).

[48] G. Genty, P. Kinsler, B. Kibler, and J. M. Dudley, "Nonlinear envelope equation modeling of sub-cycle dynamics and harmonic generation in nonlinear waveguides," Opt. Express, **15**, 5382(2007).

[49] G. P. Agrawal. *Nonlinear Fiber Optics*, 3nd edn. (San Diego, Academic, 2001).